Optimal Sensor Fusion for Structural Health Monitoring of Aircraft Composite Components

S. COSTINER, H. A. WINSTON, M. R. GURVICH, A. GHOSHAL, G. S. WELSH, S. L. BUTLER, M. R. URBAN and N. BORDICK

ABSTRACT[1]

An integrated sensor system that continuously monitors the structural integrity of an aircraft's critical composite components can have a high payoff by reducing risks, costs, inspections, and unscheduled maintenance, while increasing safety. Hybrid sensor networks combine or fuse different types of sensors. Fiber Bragg Grating (FBG) sensors can be inserted in layers of composite structures to provide local damage detection, while surface mounted Piezoelectric (PZT) sensors can provide global damage detection for the host structure under consideration. This paper describes an example of optimal sensor fusion, which combines FBG sensors and PZT sensors. Optimal sensor fusion tries to find the optimal number and location of different types of sensors such that their combined probability of detection (POD) is maximized. Optimal hybrid sensor networks can be more robust, more accurate, and/or cheaper than networks consisting only of homogenous sensors.

INTRODUCTION

Due to increased use of composites in advanced rotorcraft structures, there are strong needs for integrated health monitoring systems for damage tolerance assurance

S. Costiner, United Technologies Research Center, East Hartford, CT; Email: costins@utrc.utc.com
H. A. Winston, United Technologies Research Center, East Hartford, CT; Email: winstoha@utrc.utc.com
M. R. Gurvich, United Technologies Research Center, East Hartford, CT; Email: gurvicmr@utrc.utc.com
A. Ghoshal, U.S. Army Research Laboratory; Aberdeen Proving Ground, MD; Email: anindya.ghoshal@us.army.mil
G. S. Welsh, United Technologies Research Center, East Hartford, CT; Email: welshgs@utrc.utc.com
S. L. Butler, United Technologies Research Center, , East Hartford, CT; Email: butlersl@utrc.utc.com
M. R. Urban, Sikorsky Aircraft Corporation, Stratford, CT ; Email : murban@sikorsky.com
N. Bordick, Army Aviation Applied Technology Directorate, Fort Eustis, VA ; Email : nate.bordick@us.army.mil

[1]This research was partially funded by the US Government under Agreement No. W911W6-08-2-0002. The US Government is authorized to reproduce and distribute reprints for Government purposes notwithstanding any copyright notation thereon. The views and conclusions contained in this document are those of the authors and should not be interpreted as representing the official policies, either expressed or implied, of the Aviation Applied Technology Directorate (AATD) or the US Government.

Report Documentation Page

Form Approved
OMB No. 0704-0188

1. REPORT DATE	2. REPORT TYPE	3. DATES COVERED
SEP 2011	**N/A**	**-**

4. TITLE AND SUBTITLE
Optimal Sensor Fusion for Structural Health Monitoring of Aircraft Composite Components

5a. CONTRACT NUMBER
5b. GRANT NUMBER
5c. PROGRAM ELEMENT NUMBER

6. AUTHOR(S)

5d. PROJECT NUMBER
5e. TASK NUMBER
5f. WORK UNIT NUMBER

7. PERFORMING ORGANIZATION NAME(S) AND ADDRESS(ES)
United Technologies Research Center, East Hartford, CT

8. PERFORMING ORGANIZATION REPORT NUMBER

9. SPONSORING/MONITORING AGENCY NAME(S) AND ADDRESS(ES)

10. SPONSOR/MONITOR'S ACRONYM(S)
11. SPONSOR/MONITOR'S REPORT NUMBER(S)

12. DISTRIBUTION/AVAILABILITY STATEMENT
Approved for public release, distribution unlimited

13. SUPPLEMENTARY NOTES
See also ADA580921. International Workshop on Structural Health Monitoring: From Condition-based Maintenance to Autonomous Structures. Held in Stanford, California on September 13-15, 2011 . U.S. Government or Federal Purpose Rights License.

14. ABSTRACT
An integrated sensor system that continuously monitors the structural integrity of an aircrafts critical composite components can have a high payoff by reducing risks, costs, inspections, and unscheduled maintenance, while increasing safety. Hybrid sensor networks combine or fuse different types of sensors. Fiber Bragg Grating (FBG) sensors can be inserted in layers of composite structures to provide local damage detection, while surface mounted Piezoelectric (PZT) sensors can provide global damage detection for the host structure under consideration. This paper describes an example of optimal sensor fusion, which combines FBG sensors and PZT sensors. Optimal sensor fusion tries to find the optimal number and location of different types of sensors such that their combined probability of detection (POD) is maximized. Optimal hybrid sensor networks can be more robust, more accurate, and/or cheaper than networks consisting only of homogenous sensors.

15. SUBJECT TERMS

16. SECURITY CLASSIFICATION OF:			17. LIMITATION OF ABSTRACT	18. NUMBER OF PAGES	19a. NAME OF RESPONSIBLE PERSON
a. REPORT	b. ABSTRACT	c. THIS PAGE			
unclassified	**unclassified**	**unclassified**	**SAR**	**8**	

of these components [1-6]. A system that continuously monitors structural integrity can have a high payoff by reducing/eliminating inspections and unscheduled maintenance while increasing safety [1-15]. For example, optical Fiber Bragg Grating (FBG) sensors can be used as embedded strain sensors [9, 10] for in-situ structural health monitoring (SHM) of composite structures. In addition, significant work has been done in the area of computational modeling [7-9] and experimental testing [10-15] of embedded and surface mounted sensors in composites. A hybrid combination these sensors can provide accuracy, robustness, cost, and risk reduction advantages.

A core problem is how to combine information from different sensor types to improve damage detection. This paper proposes a generic sensor fusion approach that combines probabilities of detection (POD) of damage. A related problem is how to place sensors to maximize a fused POD - a complex global optimization problem [16, 17]. This paper demonstrates an approach based on efficient decoupled optimizations of FBG and PZT networks. The results are then combined probabilistically in POD maps. The accuracy of the solutions is evaluated by computing upper bounds of the objective. The paper is structured as follows: the physical setup and the optimization of PZT sensor networks by a greedy algorithm are described first. This PZT optimization is similar to the FBG optimization described in [1]. These two optimizations are combined in an optimal sensor fusion approach. POD maps and applications of the optimization are discussed in the last section.

DESCRIPTION OF THE PHYSICAL SETUP

This section describes the damage detection model. A helicopter composite flexbeam is composed of a set of plies or layers. The flexbeam is a safety critical component that is highly loaded and susceptible to cracks. In this study, it is assumed that cracks can only develop at ply drop locations (i.e., at the ends of plies that terminate in the interior of the structure), as shown in Figure 1. There are N_p plies in the sample labeled with an index

Cracks: A crack $c = (x_c, y_c, \alpha)$ is defined by its coordinates (x_c, y_c) and length α. Here, (x_c, y_c) is the location of the beginning of the crack, where x_c is the radial coordinate down the length of the flexbeam, and y_c is the transverse coordinate through the thickness of the flexbeam. A set of possible cracks or delaminations is denoted by $\boldsymbol{C} = \{(x_c, y_c, \alpha)\}$. It is assumed that all cracks have the same size $\alpha = 1.5$ inches. We assume that $|C|$ equals the number of plies that terminate at ply drops. P(c) denotes the probability of having a crack $c = (x_c, y_c, \alpha)$ and was assumed to be 0.035.

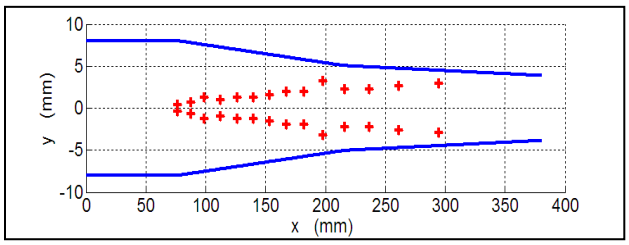

Figure 1. Flexbeam Cross Section;
Ply Drops (red crosses) are Possible Crack Locations.

It was also assumed that the sum of all P(c) values is less than or equal to unity. Although, in principle, multiple damage sites can exist in a component, in this paper it is assumed that either no cracks or only a single crack exists in a flexbeam.
Loading: The sensor network was optimized for a static load generated by a flexbeam tip deflection d of 3.00 inches. For simplicity, the fixed crack length α and tip deflection d are implicit in the rest of this paper.
Sensors: PZT sensors are positioned on the surface of the component. FBG sensors are positioned on fibers inside the component along plies.

PZT SENSOR OPTIMIZATION

The goal of PZT optimization is to find surface-mounted sensor positions that maximize the probability of detecting interior cracks. This optimization is similar to FBG sensor optimization described in [1]. PZT devices are positioned on the surface of the sample along the length of the flexbeam. The position of a PZT device is denoted by the x coordinate of the beginning (i.e., left-hand side) of that device. Given two PZT devices positioned at x_1 and x_2, the device at x_1 acts as an actuator that sends a signal into the sample that is received by the device at $x_2 > x_1$. For a given crack $c = (x_c, y_c, \alpha)$, the probability of detecting this crack by the PZT device pair (x_1, x_2) is denoted by $P(x_1, x_2, c)$. $P(x_1, x_2, c)$ is computed from an analytic model created by fitting data from acoustic wave propagation simulations where reflected amplitude maxima were monotonically mapped to probabilities of detection.

The length L of the flexbeam is divided into equal-sized elements. Each PZT actuator or receiver is located at one of these elements and occupies a whole number λ_{PZT} of elements. A PZT sensor consists of an actuator and a receiver separated by a fixed distance d_0. Hence, the POD $P(x_i, x_j, c) = P(x_i, c)$ is only a function of the actuator location x_i. The minimum distance between two consecutive PZT sensors is specified as a given number of elements d_{min}.

The probability that a set of PZT sensors, located at $\vec{x} \equiv (x_1,\ldots,x_n)$, detects a crack c is given by:

$$POD_{PZT}(\vec{x}, c) = [1 - \prod_{i=1,n} (1 - P(x_i, c))] \cdot P(c) \qquad (1)$$

For a given set of cracks C, the optimization objective is given by:

$$POD_{PZT}(\vec{x}, C) = \sum_{c \in C} POD_{PZT}(\vec{x}, c) \qquad (2)$$

This is the average probability of detecting a crack in C. It is referred to as the exact objective or exact probability of detection POD_{PZT} to distinguish it from approximate objectives denoted by POD'_{PZT}. The sensor optimization problem is to find a set of n PZT sensor locations $\vec{x}^* \equiv (x_1^*,\ldots,x_n^*)$ such that:

$$\vec{x}^* = \arg\max_{\vec{x}} POD_{PZT}(\vec{x}, C) \qquad (3)$$

$$|x_i - x_j| \geq \lambda_{PZT} + d_{min};\ i, j = 1,\ldots, n,\ i \neq j \qquad 0 \leq x_i \leq L - \lambda_{PZT};\ i = 1,\ldots, n$$

The above is a complex global optimization problem that has many local maxima. The next section describes an efficient greedy algorithm for finding good initial solutions using an approximate objective POD'_{PZT}. These approximate solutions can be evaluated by the exact objective. If the value of the exact objective POD_{PZT} is not satisfactory (e.g., it is not sufficiently close to 1 or to a computed upper bound), then the approximate solution can be further improved by continuous local optimization.

Greedy Algorithm

The optimization problem, defined by Equation 3, can be solved by a greedy algorithm that is similar to the procedure used to optimize FBG sensor networks in [1]. The approach is to first define an approximate objective for each element location x_i as an average probability of detecting all the cracks in ***C*** with a PZT sensor at that position.

$$POD'_{PZT}(x_i) = \sum_{c \in C} P(x_i, c)P(c) \tag{4}$$

The first PZT sensor is positioned at x_1^* - the location of the largest value of POD'_{PZT}.

$$x_1^* \equiv \underset{x_i}{\text{argmax}}\ POD'_{PZT}(x_i) \tag{5}$$

The second sensor is positioned at the location of the next largest feasible value of POD'_{PZT}, such that $|x_1 - x_2| \geq \lambda_{PZT} + d_{min}$. This procedure continues positioning additional sensors in the same way and was used to determine the seven optimal PZT sensor positions shown in Figure 2. The numbers denote the order in which the sensors were placed, and the vertical lines show the locations of the ply drops. The exact objective POD_{PZT} was evaluated for one to ten sensor greedy algorithm solutions. The results are shown in Figure 3. As expected, the detection probability increases with the number of sensors. For six or more sensors, the POD curve saturates because additional sensors would have to be positioned in regions where POD'_{PZT} vanishes, as seen in Figure 2.

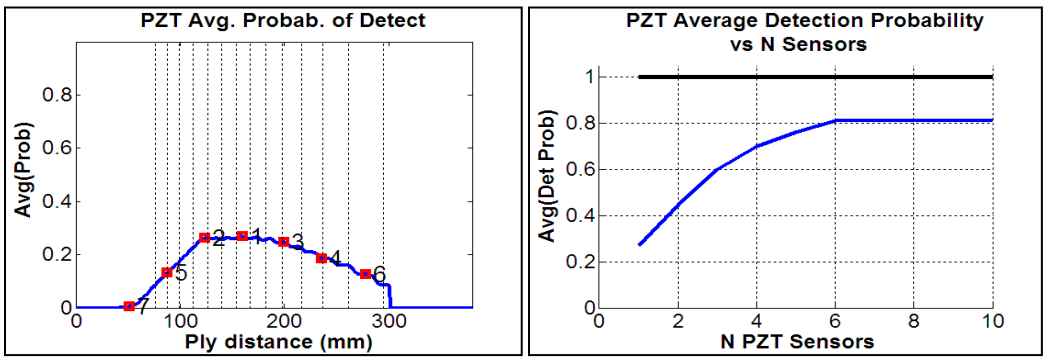

Figure 2 (left). Approximate Objective POD'_{PZT} and a 7 PZT Sensor Greedy Solution (Ply 12).
Figure 3 (right). Exact Objective POD_{PZT} Applied to Greedy Solutions vs. Number of PZT Sensors in Ply 12 (blue curve).

HYBRID SENSOR FUSION

This section defines a hybrid sensor fusion formulation using POD objective functions. Assume that there are n PZT sensors at locations $\vec{x}$ and m FBG sensors at locations $\vec{g}$. Analogous to the FBG greedy optimization problem, the combined POD of the two sets of sensors is given by the exact objective function:

$$POD_{FBGx\ PZT}(\vec{x},\vec{g},C) = \sum_{c\in C} P(c)\cdot[1-\prod_{i=1,n}(1-P(x_i,c))\prod_{j=1,m}(1-P(g_j,c))] \tag{6}$$

This objective function can be approximated by a separable objective $POD^{sep}_{FBGxPZT}$ given by Equation 7. (POD_{FBG} is given by an equation similar to Equation 1.)

$$POD^{sep}_{FBGxPZT}(\vec{x},\vec{g},C) = 1-(1-POD_{PZT}(\vec{x},C))\cdot(1-POD_{FBG}(\vec{g},C)) \tag{7}$$

The separable objective $POD^{sep}_{FBGxPZT}$ was used because POD_{FBG} and POD_{PZT} could be evaluated independently. This enabled the PZT and FBG optimizations to be decoupled. The formulation of Equation 7 can be extended to other types of sensors for which a POD can be computed. It can also be extended to any number of different types of sensors.

POD Bounds and Error Estimates

The above objectives have computable upper bounds. For example, denoting by N the total number of elements x_i on which PZT sensors can be located, and by M the total number of elements g_i on which FBG sensors can be located, the inequality in Equation 8 holds for any n and m.

$$POD_{FBGxPZT}((x_1,...,x_n,g_1,...,g_m),C) \le \sum_{c\in C}[1-\prod_{i=1,N}(1-P(x_i,c))\prod_{j=1,M}(1-P(g_j,c))]\cdot P(c) = U_{bd} \tag{8}$$

If $(\vec{x}^*,\vec{g}^*)$ is a global maximum of $POD_{FBGxPZT}(\vec{x},\vec{g},C)$, and $(\vec{x},\vec{g})$ is a solution obtained by any other procedure, then the bounds in Equation 9 hold:

$$L_{bd} \equiv POD_{FBGxPZT}(\vec{x},\ \vec{g},\ C) \le POD_{FBGxPZT}(\vec{x}^*,\vec{g}^*,C) \le U_{bd} \tag{9}$$

Equation 9 provides upper and lower bounds of the global optimum of the exact objective $POD_{FBGxPZT}$. Hence, the difference $U_{bd} - L_{bd}$ provides an error estimate of the global optimum. For example, the upper bound U_{bd} is represented by the horizontal black line, and the lower bound is represented by the blue curve in Figure 3. Here, the number of FBG sensors is 0 because only PZT sensors were used. Note that, in some cases, the upper bound U_{bd} can be less than one.

Complete Problem Formulation

The complete hybrid sensor optimization problem is expressed by Equation 10. The problem is to find n PZT sensor locations $\vec{x}^* \equiv (x_1^*,\ldots,x_n^*)$ and m FBG sensor

locations $\vec{g}^* \equiv (g_1^*, \ldots, g_m^*)$ that maximize $POD_{FBGxPZT}(\vec{x}, \vec{g}, C)$. Solutions must satisfy feasibility bounds and constraints (i.e., the FBG sensors cannot be positioned at locations where they could be damaged by peak strain fields). Here, λ_{FBG} is the FBG sensor size, and b_{min} is the minimum distance between FBG sensors.

$$
\begin{aligned}
(\vec{x}, \vec{g})^* &= \arg\max_{\vec{x}, \vec{g}} POD_{FBGxPZT}(\vec{x}, \vec{g}, C) \qquad (10)\\
|x_i - x_j| &\geq \lambda_{PZT} + d_{min} \qquad i, j = 1, \ldots, n \quad i \neq j\\
|g_i - g_j| &\geq \lambda_{FBG} + b_{min} \qquad i, j = 1, \ldots, m \quad i \neq j\\
0 \leq x_i &\leq L - \lambda_{PZT} \qquad i = 1, \ldots, n\\
0 \leq g_i &\leq L - \lambda_{FBG} \qquad i = 1, \ldots, m
\end{aligned}
$$

Approximate solutions to this problem can be found by independently optimizing the PZT and FBG sensor networks with greedy approaches. These solutions can then be evaluated with the separable objective function $POD^{sep}_{FBGxPZT}$ and the exact objective function $POD_{FBGxPZT}$. If the computed POD values found by such a procedure do not meet engineering requirements, the solutions can be improved either iteratively or by local optimization. If the exact objective $POD_{FBGxPZT}$ is close to 1 or to the computed upper bound U_{bd}, then the solution can be considered to be close to a global optimum. The results shown below were obtained by this approximate optimization procedure.

Example Solutions

Objective functions for combined FBG and PZT sensor networks are shown in Figure 4 (separable) and Figure 5 (exact). These are referred to as optimal POD maps and are similar in this case. The relative difference between the separable and exact PODs is shown in Figure 6 and is defined as $(POD_{FBGxPZ} - POD^{sep}_{FBGxPZT}) / POD_{FBGxPZT}$. The relative difference approaches 0 as the number of sensors increases. Note that the maximum $POD_{FBG} \sim 0.55$ and the maximum $POD_{PZT} \sim 0.8$, while the hybrid solutions give a maximum $POD_{FBGxPZT} \sim 0.9$. Hence, the combination of the two types of sensors gives a higher POD than a network with only one type of sensor. This can be understood from objective function distributions. In particular, although not shown, the PZT objective function has large values in the center of the flexbeam where the FBG objective values vanish.

APPLICATIONS OF OPTIMAL SENSOR FUSION

Combined PZT and FBG optimal POD maps can be used to answer three main classes of problems. (1) For given numbers of FBG and PZT sensors, what sensor configuration(s) achieve the maximum attainable POD? For example, with seven PZT and seven FBG sensors in ply 12, a lower bound of the maximum value of $POD_{FBGxPZT}$ is 0.9, as shown in Figure 5. (PZT solutions that give this POD are shown in Figure 2.) In general, these solutions are not unique. (2) How many PZT and FBG sensors are needed to achieve a given target POD? What are the corresponding sensor configurations? For example, for a target POD of 0.85 in ply 12, six FBG and five PZT sensors or five FBG and six PZT sensors would be sufficient (Figure 5). These

solutions can be obtained by selecting the best five or six sensor positions from the approximate PZT objective curve in Figure 2 and a corresponding FBG approximate objective curve. (3) What is the minimum number of sensors that give the maximum (or a given) POD? For example, six PZT and six FBG sensors provide the maximum POD value of 0.9 in the case illustrated in Figure 5.

CONCLUSIONS

A generic sensor fusion approach that combines the POD(s) of heterogeneous sensors was described. In particular, an optimal sensor fusion approach was defined and demonstrated on hybrid FBG and PZT sensor arrays. Computable lower and upper error bounds of a POD objective function were determined. The optimization approach combines the optimization of FBG networks with the optimization of PZT networks. PZT sensor network optimization uses a greedy algorithm that is combined with an analytical model that computes delamination detection probabilities for pairs of PZT devices. The optimization approach can be used to distinguish situations where hybrid heterogeneous sensor networks are better than homogeneous sensor networks.

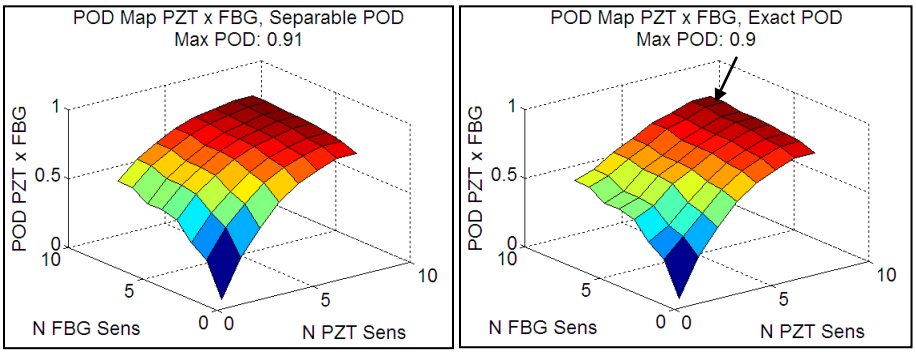

Figure 4 (left). Separable Objective Map of Greedy Solutions for PZT and FBG Sensors (Ply 12).
Figure 5 (right). Exact Objective Map of Greedy Solutions for PZT and FBG Sensors (Ply 12).

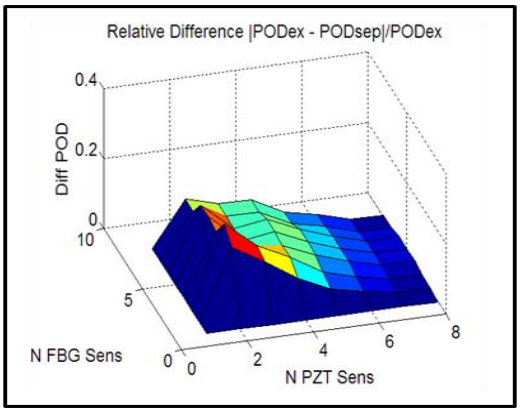

Figure 6 (bottom). Relative Difference between Separable and Exact Objectives (Ply 12).

REFERENCES

1. Ghoshal, A., G.S. Welsh, M.R. Gurvich, S.L. Butler, H.A. Winston, S. Costiner, P. Attridge, M.R. Urban, N. Bordick. 2010. "Smart Embedded Sensors in Rotorcraft Composite Components for Condition Based Maintenance", American *Helicopter Society 66th Annual Forum*, Phoenix, AZ, May 11-13, 2010.
2. Butler S.L., A. Ghoshal, M.R. Gurvich, G.S. Welsh, M.R. Urban, N. Bordick. 2010. "Analysis of Interlaminar Damages in Thick Rotorcraft Composite Components with Embedded Sensors." *American Helicopter Society 66th Annual Forum*, Phoenix, AZ, May 11-13, 2010.
3. Baker A., S. Dutton, D. Kelly. 2004. *Composite Materials for Aircraft Structures*. American Institute of Aeronautics and Astronautics, 2nd ed.
4. Garg D.P., M.A. Zikry, G. Anderson. 2001. "Current and potential research activities in adaptive structures, An ARO perspective". *Smart Materials Structures*, Vol.10, 2001, pp. 610-623.
5. Schulz M.J., P.F. Pai, D.J. Inman. 1999. "Health Monitoring and active control of composite structures using peizoceramic patches". *Composites Part B: Engineering*. Vol 30, Issue 7, October 1999, pp. 713-725.
6. Ghoshal A., J. Harrison, M.J. Sundaresan, D. Hughes, M.J. Schulz. 2002. "Damage detection on a helicopter flexbeam". *Journal of Intelligent Materials Systems and Structures*. Vol,. 12, No 5, 2002, pp 315-330,
7. Butler S.L, M. Gurvich, A. Ghoshal, G. Welsh, N. Bordick. 2009. "Health Monitoring of Thick Composite Rotorcraft Components: Effect of Embedded Sensors on Interlaminar Damage Process". *AHS International National Technical Specialists' Meeting on Rotorcraft Structures and Survivability*. Williamsburg, VA, October 27-29, 2009.
8. Liu W., V. Giurgiutiu. 2007. "Finite Element Simulation of Piezoelectric Wafer Active Sensor for Structural Health Monitoring with Coupled-Filed Element". *Proceedings of SPIE, the International Society for Optical Engineering*. 2007; Vol. 6529 (2), pp. 65293R.1-65293R.13
9. Kim H.S., A. Ghoshal, A. Chattopadhyay, W.H. Prosser. 2004. "Development of Embedded Sensor Models in Composite Laminates for Structural Health Monitoring". *Journal of Reinforced Plastics and Composites*. 2004; Vol. 23, No. 11, pp. 1207-1240
10. Meltz, G., W.W. Morey, W.H. Glenn. 1989. "Formation of Bragg gratings in optical fibers by a transverse holographic method". *Optical Letters* 14, 1989, pp. 823-825.
11. Park J.W., C.Y. Ryu, H.K. Kang, C.S. Hong. 2000. "Detection of buckling and crack growth in the delaminated composites using fiber optic sensor". *Journal of Composite Materials*, Vol. 34, No. 19, 2000, pp. 1602-1623
12. Chang F.K., J.F.C. Markmiller, J.B. Ihn, K.Y. Cheng. 2007. "A Potential Link from Damage Diagnostics to Health Prognostics of Composites through Built-in Sensors". *Transaction of the ASME*. Vol. 129, December 2007, pp. 718-729
13. Kusaka T., P.X. Qing. 2003. "Characterization of Loading Effects on the Performance of SMART Layer Embedded or Surface-Mounted on Structures". *Proceeding of the Fourth International Workshop on Structural Health Monitoring, Stanford University*. 2003, pp. 1539-1546.
14. Ghoshal A., W.H. Prosser, H.S. Kim, A. Chattopadhyay, B. Copeland. 2010. "Development of embedded piezoelectric acoustic sensor array architecture". *Microelectronics Reliability*, 2010.
15. Asanuma H., O. Haga, J. Ohira, G. Hakoda, K. Kimura. 2002. "Proposal of an active composite with embedded sensor". *Science and Technology of Advanced Materials*. Vol 3. #2., 2002.
16. COCONUT Project. 2001. *Algorithms for Solving Nonlinear Constrained Optimization Problems: The State of the Art*. http://www.mat.univie.ac.at/~neum/glopt/coconut/2001
17. Pinter J. (Ed). 2006. *Global Optimization: Scientific and Engineering Case Studies (Nonconvex Optimization and Its Applications)*. Springer, 2006